Computers in Biology and Medicine 132 (2021) 104302

Contents lists available at ScienceDirect

Computers in Biology and Medicine

journal homepage: http://www.elsevier.com/locate/compbiomed

# An exploratory investigation of patellofemoral joint loadings during directional lunges in badminton

Lin Yu [a,b,c], Qichang Mei [c,d,**], Nur Ikhwan Mohamad [b], Yaodong Gu [c,d,*], Justin Fernandez [c,d,e]

[a] Loudi Vocational and Technical College, Loudi, China
[b] Faculty of Sports Sciences and Coaching, Sultan Idris Education University, Tanjong Malim, Malaysia
[c] Faculty of Sports Science, Ningbo University, Ningbo, China
[d] Auckland Bioengineering Institute, University of Auckland, Auckland, New Zealand
[e] Department of Engineering Science, University of Auckland, Auckland, New Zealand

ARTICLE INFO

*Keywords:*
Lunge
Patellofemoral cartilage
OpenSim
Finite element analysis

ABSTRACT

Anterior knee pain is a commonly documented musculoskeletal disorder among badminton players. However, current biomechanical studies of badminton lunges mainly report kinetic profiles in the lower extremity with few investigations of in-vivo loadings. The objective of this study was to evaluate tissue loadings in the patellofemoral joint via musculoskeletal modelling and Finite Element simulation. The collected marker trajectories, ground reaction force and muscle activation data were used for musculoskeletal modelling to compute knee joint angles and quadricep muscle forces. These parameters were then set as boundary conditions and loads for a quasistatic simulation using the Abaqus Explicit solver. Simulations revealed that the left-forward (LF) and backward lunges showed greater contact pressure (14.98–29.61%) and von Mises stress (14.17–32.02%) than the right-forward and backward lunges; while, loadings in the left-backward lunge were greater than the left-forward lunge by 13–14%. Specifically, the stress in the chondral layer was greater than the contact interface, particularly in the patellar cartilage. These findings suggest that right-side dominant badminton players load higher in the right patellofemoral joint during left-side (backhand) lunges. Knowledge of these tissue loadings may provide implications for the training of badminton footwork, such as musculature development, to reduce cartilage loading accumulation, and prevent anterior knee pain.

## 1. Introduction

The lunging step is a unilateral motion involving upper and lower limbs of the same side, which is commonly performed in several sports, such as badminton, fencing, squash, and other general exercise training. Specifically, in badminton, this motion represents over 15% of all badminton movements in singles male competition [1], apart from jumps and cutting manoeuvres. It has been reported there are over 52.2 moves of the half lunge and 46.1 moves of the forward lunge per match [2]. Badminton is the fastest racket sport with over 200 million participants around the globe [3]. Several researchers have focused on the biomechanics of badminton techniques to identify areas of improving performance and preventing injuries [4], investigating different motion techniques (kick, step-in and hop) [1], directional (or diagonal) lunges (moving from central court base position towards right-forward, left-backward, right-backward and left-backward) [5], athletic-level based lunge performance [6], and single versus repeated lunges [7].

In terms of badminton injuries, the knee joint is a highly documented injured site in the lower extremity [8,9]. It has been reported as an overuse injury due to the accumulated loadings from training or practice sessions [10]. The main documented injury types for the knee were patellofemoral joint pain syndrome [9], and patella tendinopathy [11,12]. The patella normally functions as a lever to direct the quadriceps during knee extension. The peak force produced by the quadriceps during concentric contraction and time to peak force was reported to be key indicators of lunge performance, specifically a quicker completion of lunge and return to the start position in badminton [13,14]. Disorders (pain or injury) to the anterior knee affects the normal lunge motion, thus reducing athletic performance, or even limiting knee flexion/extension motions.

* Corresponding author. Faculty of Sports Science, Ningbo University, No. 818, Fenghua Rd, Jiangbei District, Ningbo, Zhejiang, 315211, China.
** Corresponding author. Faculty of Sports Science, Ningbo University, No. 818, Fenghua Rd, Jiangbei District, Ningbo, Zhejiang, 315211, China.
*E-mail addresses:* meiqichang@outlook.com (Q. Mei), guyaodong@hotmail.com (Y. Gu).

https://doi.org/10.1016/j.compbiomed.2021.104302
Received 12 October 2020; Received in revised form 25 February 2021; Accepted 25 February 2021
Available online 2 March 2021

Patellofemoral pain is a commonly reported knee problem [15,16], not only observed in badminton players. It is also known as "runners' knee", due to the quantity of reports in runners [17,18]. A normally functioned patellofemoral joint requires a suitable articulation surface between the femoral trochlear and patellar facet, balanced soft tissue structures, and equal pulling quadriceps forces [19]. Any malfunction in this system would lead to a gradual onset of anterior knee pain, especially during dynamic activities, such as squatting, running, climbing and lunging [18]. Traditional 2D analytical models [20], and current 3D musculoskeletal models have been used to investigate in vivo mechanical loadings, such as shear stress and pressure [21,22], within this complex structure. A comprehensive framework integrated computational modelling from reconstructed magnetic resonance images (MRI) and muscle forces from experimental tests to estimate the patellofemoral joint cartilages stress [23]. This approach revealed that contact area increased by 24% during knee flexing to 60° [24], and higher cartilage stress and smaller contact area in females with patellofemoral pain [25].

In terms of badminton lunges, a recent review summarized the key attributes to the performance of lunges, covering kinematic and kinetic parameters [26,27]. Specifically, the left-forward backhand lunge presented greater impact magnitude compared to other lunging directions [5]. The higher impact loading rate and peak knee flexion moment may explain overuse injuries [28]. A greater peak knee anterior-posterior force and flexion moment were found in the single left forward lunge while comparing to repeated left forward lunges, which was due to shorter contact time and smaller maximal loading rate and impact force from repeated lunge [7]. Athletes with knee pain were found to present conservative movements with reduced knee and trunk motion as a compensation strategy [29]. Different lunging types (such as kick, step-in and hop) also exhibited different loading profiles and mechanical output in the lower extremity [1], specifically, the kick lunge placed more mechanical loading in the lower extremity and step-in lunge was adopted for increased distance, while the hop lunge increased force output assisting with lunging recovery. While loading profiles were reported, the variance in kinematics may be due to the different lab setup and experimental conditions [27].

Computer-aided technologies and approaches are gradually playing key roles for badminton lunge research, improving prevention of potential injuries [26]. However, the in-vivo tissue loadings during badminton lunges have been scarcely reported in the literature. Based on current knowledge about patellofemoral pain, the primary objective of this study was to investigate the loadings, specifically the contact pressure and von Mises stress, distributed in the femur and patella cartilage while performing a single maximal lunge toward the directions of right-forward, right-backward, left-forward, and left backward in a lab-simulated badminton court. It was hypothesized that the left-side (forward and backward) lunges would have greater loadings in the cartilage than the right-side lunges. A second objective was to reveal the differences in contact pressure and von Mises stress magnitudes in the four directional lunges.

## 2. Methods

### 2.1. Participants and experimental protocol

A total of 12 male badminton athletes (age: 20.5 ± 3.1yrs, height: 176 ± 4.9 m, mass: 68.6 ± 5.6 kg) from a local badminton club joined this test. The right (upper & lower) limb was determined as the dominant side during the participants inclusion. They all had experience of playing badminton for over 5 years. No injuries were reported in the past six months prior to the test. The study was approved by the institutional ethical committee in the University following the Declaration of Helsinki. Participants were informed of the objectives, procedures, and requirements concerning the test with consent.

Directional lunges were conducted in a gait lab, with an eight-camera Vicon motion capture system (Oxford Metrics Ltd., Oxford, UK) and embedded AMTI force plate (Watertown, MA, United States), enabling the synchronous collection of marker trajectories and ground reaction force. The frequency for collecting maker trajectories and ground reaction forces were set at 200 Hz and 1000 Hz, respectively. The lunges were performed in a lab-simulated court via adjusting positions of the net as the force plate was fixed in ground (Fig. 1A). During the experiment, participants initiated with the left foot stepping forward at position (***1***) and finished lunging with the right foot at position (***2***) onto the force plate towards the right forecourt, left forecourt, right backcourt, and left backcourt. This was defined as a 'kick' lunge with the dominant leg accepting the weight as per the classification in a previous study [1]. The lunging motions were separately defined as the Right (forehand)-Forward (**RF**), Right(forehand)-Backward (**RB**), Left (backhand)-Forward (**LF**) and Left(backhand)-Backward (**LB**) lunging steps. The motion followed our previously established protocol [6] in the lab-simulated court (Fig. 1A). Similar protocols were adopted in several recent studies of badminton lunge [5,7,28].

As illustrated in Fig. 1B, the marker set included bilateral Acromion, ASIS, PSIS, thigh-cluster, med/lat knee (epicondyle), lower patella, tibial tuberosity, shank-cluster, med/lat ankle (malleoli), calcaneus, first/third/fifth metatarsals, and the big toe tip. Muscle activities of the vastus medialis (***VM***), rectus femoris (***RF***) and vastus lateralis (***VL***) were recorded using a wireless surface EMG system (Delsys, Boston, MA, United States) at a frequency of 1000 Hz, which was used to validate against the estimated muscle activation and muscle forces. The raw signals from surface EMG were firstly filtered with a fourth-order low-pass band, then via a root mean square (RMS) analysis, and lastly normalized to the peak activation from the maximal voluntary contractions of the quadriceps muscles. The activities of the quadriceps were expressed as 0 (no activity) ~ 1 (fully activated) to compare against the estimated activation from musculoskeletal modelling.

A musculoskeletal model with one degree of freedom (flexion/extension) at the knee joint, which prescribed patella motion with knee flexion, was adopted in this study [30]. An established pipeline [31–33] was followed during musculoskeletal modelling. The initial step of '***Scaling***' was performed to obtain anthropometric-matched models with adjusted muscle attachments, length properties and moment arms. The '***Inverse Kinematics***' was then conducted to calculate knee joint flexion angle with minimized position errors between virtual model markers and experimental makers. A '***Static Optimization***', which minimized the sum of muscle activation squared [30,33,34], was employed to compute the muscle activations and muscle forces for the four directional lunges in OpenSim 3.3 (Fig. 2a). The knee flexion angles and validated muscle (vastus medialis, rectus femoris, vastus intermedius and vastus lateralis) forces (Fig. 2*b*) were used as boundary conditions and loads for the Finite Element simulation.

### 2.2. Model development

One participant attended an MRI scanning session at the local hospital to collect the geometry of their bones and cartilage in the knee joint complex using a 3.0-T SIEMENS MR system. The T1 VIBE weighted fat-suppressed images of the sagittal and coronal planes were obtained (repetition time: 4.11 ms; eco time: 1.23 ms; slice thickness: 1 mm; field of view: 81.25 mm; and matrix: 320x260). The images were imported into Mimics version 21 (Materialise, Leuven, Belgium) for manual segmentation of the femur, patella and tibia bones, and femur and patella cartilage (Fig. 2*c*), which were further wrapped and smoothed in Mimics before exporting as ***stl*** geometry files (Fig. 2*d*). The ***stl*** geometries were meshed in the HyperMesh (Hyperworks 2017, Altair, USA) software.

Specifically, the femur and patella bones were meshed as hexahedral elements with element size of 1 mm, the tibia bone was meshed as tetrahedral elements with element size of 1 mm. The femur and patella cartilage were meshed as hexahedral elements with element size of 0.5 mm, as a recent mesh convergence study reported that mesh size between 0.5 and 0.75 mm did not alter contact pressure and stress

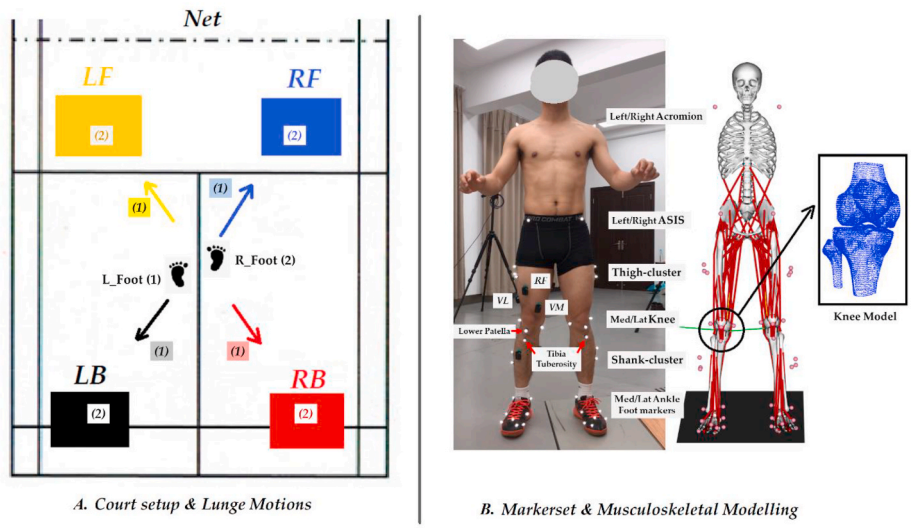


**Fig. 1.** An illustration of lab-simulated court and musculoskeletal setup in this study.

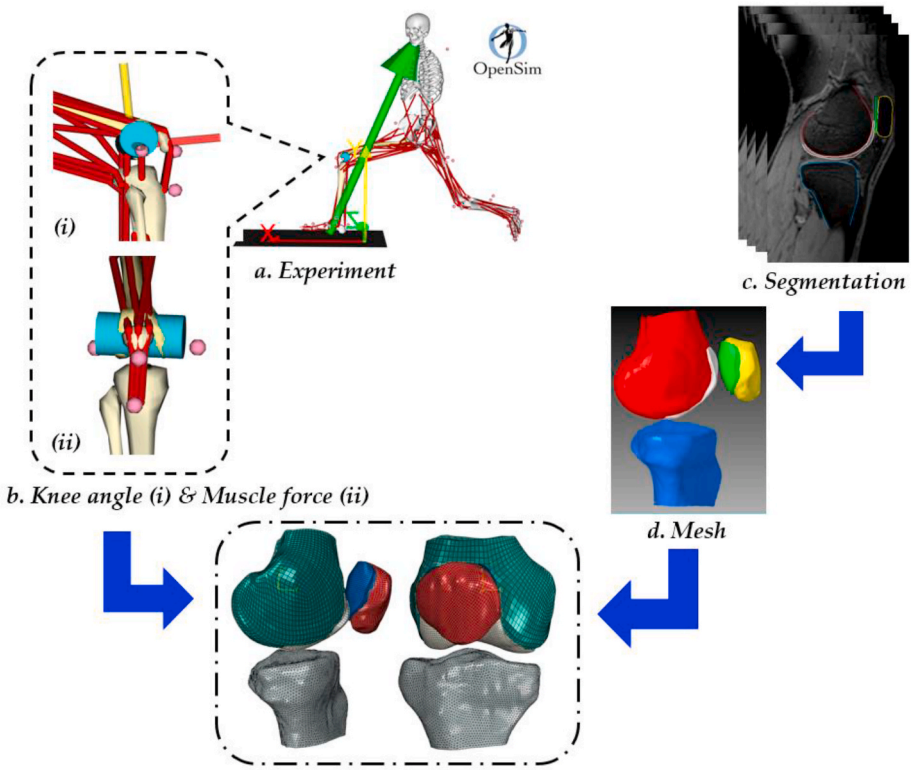


**Fig. 2.** An outline of experimental (***a, b***) and computational (***c, d***) workflow in this study.

significantly but may require longer computing time [35]. All meshed bone and cartilage geometry files were exported as ***inp*** files for model assembly and FE simulation. The femur, patella and tibia bones were treated as rigid bodies, while a linear elastic isotropic material property of Young's Modulus of 12Mpa and Poisson's ratio of 0.46 were assigned to the femur and patella cartilage [25]. The articulated femur cartilage was attached to the femur bone using 'tied' constraints as a slave surface to master surface discretization, and the same approach was employed for the patella cartilage and patella bone.

Following the positions of markers on the lower patella and tibia tuberosity from this participant during motion capture, the patella tendon was simulated using three tension-only linear elements of axial connectors with a stiffness of 2000 N/mm to connect the patella with the tibia tuberosity [25,36]. The quadriceps were modelled as tension-only axial connectors for the vastus medialis (**VM**) (three elements), vastus intermedius (**VI**) (three elements), rectus femoris (**RF**) (three elements) and vastus lateralis (**VL**) (three elements) to connect the patella bone. The attachment points were identified from the MRI images, while the orientation of VI and RF were set as parallel to the long axis of the femur, and the VM and VL oriented to the medial and lateral borders of the quadriceps as determined from MRI images of this participant [35,37]. Estimated quadriceps muscle forces from static optimization in OpenSim musculoskeletal modelling were input as connector forces for the FE simulation.

### 2.3. Finite Element simulation

Following a previously established workflow [23], a quasi-static loading simulation for the four lunging steps was conducted using the Abaqus Explicit solver (Abaqus/CAE 2017, Simulia, Dassault Systemes, Johnston, RI, USA) in the current model. While simulating the four directional lunges, the calculated mean angle of knee flexion was set as boundary conditions to position the tibia and femur while the patella was translated anteriorly for a gap between cartilages [25,35]. The estimated muscle forces of the quadriceps (specifically, vastus medialis, ***VM***; vastus intermedius, ***VI***; rectus femoris, ***RF***; and vastus lateralis, ***VL***) were applied as connector forces to pull the patella towards the femur. The proximal end of the femur and distal end of the tibia bones were fixed with no degree of freedom as boundary conditions, and the patella was set free with six degrees of freedom. The contact relationship between the patella cartilage surface and femur cartilage surface was defined using a penalty-based hard contact pressure-overclosure [38]. The contact pressure represents the magnitude of stress that uniformly distributed to compress the cartilage at the surface, while the von Mises stress represents the portion to distort or deform the cartilage tissue [35]. The peak contact pressure at the surface and von Mises stress at the centroid of the surface (patellar cartilage and femur cartilage interface) and chondral (cartilage and bone interface) elements were used to quantify the stress in contact between the patella and femur cartilage. The von Mises stress in the central region of the cross-sectional interface in the patellofemoral groove was presented.

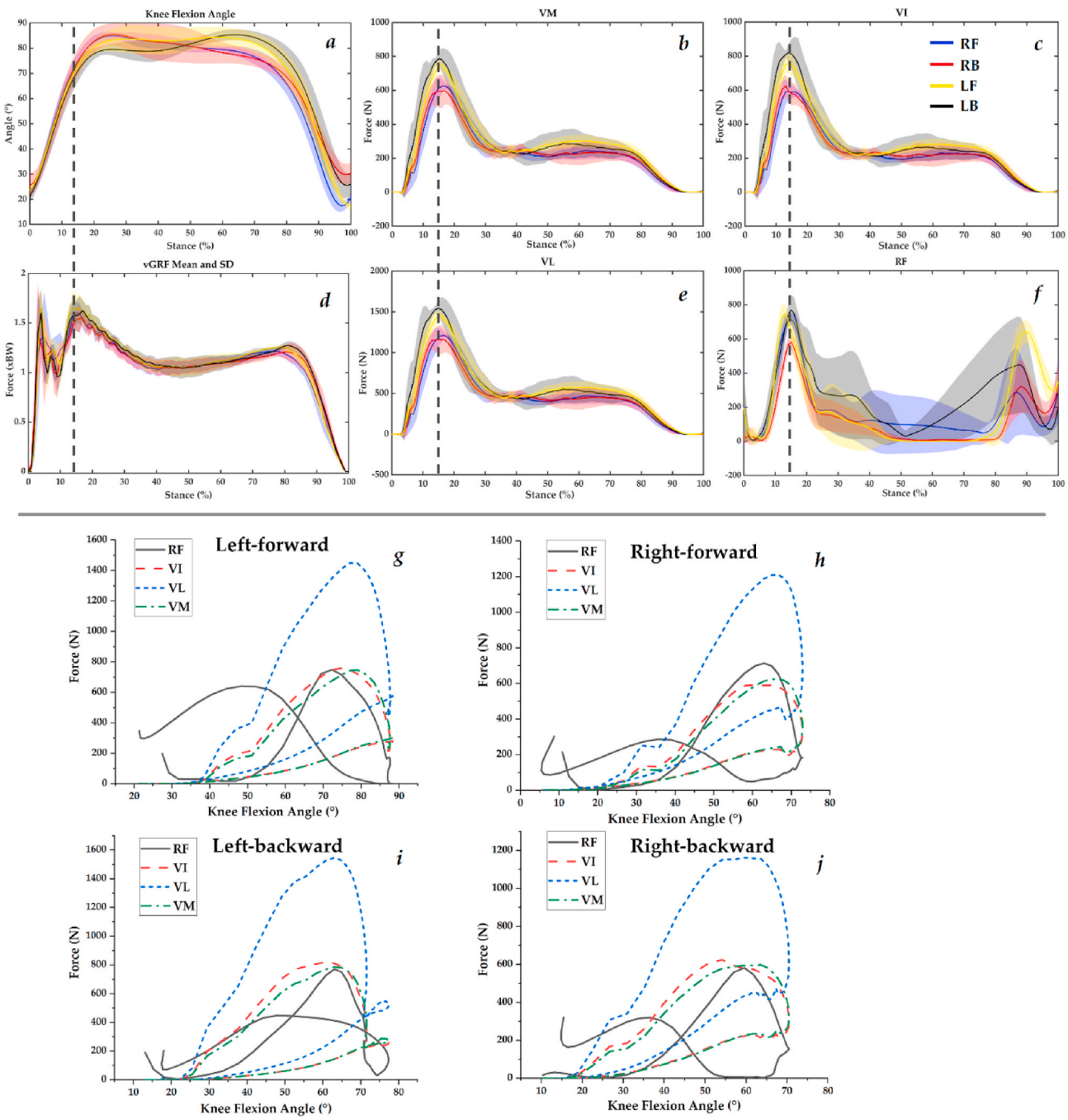


**Fig. 3.** Illustration of the knee flexion angles (*a*), vertical ground reaction forces (*d*), and quadriceps (*b*: VM, *e*: VL, *c*: VI, *f*: RF) forces in mean and standard deviation, and mean flexion angles against mean quadriceps forces (*g, h, i, j*) during the four directional lunges.

## 3. Results

### 3.1. Model evaluation

As presented in Fig. 3, the knee flexion angle waveforms during lunging stance from all 12 participants are compared against recent studies of badminton lunging steps [1,6,39] showing similar motion patterns. While defining the knee position of this specific participant with knee scanned for FE modelling, the mean angles of 65° (RF), 60° (RB), 79° (LF), and 63° (LB) are determined with peak impact from the vertical ground reaction force (highlighted with dashed line in Fig. 3). The quadriceps muscle forces versus the knee flexion angles are presented to facilitate the selection of input parameters for the FE simulation. Specific parameters of the knee angle and quadricep forces for the FE simulation are presented in Table 1 (quadriceps muscle forces in Newtons, body weight normalized in BW).

To evaluate our musculoskeletal and FE models, the estimated peak quadriceps muscles activations are firstly compared against experimental EMG signals of the normalized muscle activities to the activities from maximum voluntary contraction (MVC) (Fig. 4). Further, the contact area between the femur cartilage and patella cartilage predicted from FE simulation in the four directional lunges were 565.2 $mm^2$ (**RF**, right-forward), 515.4 $mm^2$ (**RB**, right-backward), 585.9 $mm^2$ (**LF**, left-forward) and 620.9 $mm^2$ (**LB**, left-backward), respectively. These values are similar with the reported contact area of 500–600 $mm^2$ with weight-bearing knee flexion (~60°) observed in a recent study [24].

### 3.2. Contact pressure

Fig. 5 illustrates the overall contact pressure distribution on the femoral and patella cartilages during LF, LB, RF and RB lunges. The pressure is focalized in the central and lateral facets of the femoral cartilage, while the pressure is consistent across the medial-to-lateral facet of the patella cartilage. Specifically, the LB lunge presents larger contact pressure than the LF and RF lunges, followed by a smaller magnitude of contact pressure observed in the RB lunge. Specifically, the discrete peak values are 25.5 MPa (LB), 22.12 MPa (LF), 17.95 MPa (RB) and 21.68 MPa (RF), respectively. The largest contact pressure is observed in the LB lunging step, followed by reduced pressure in the LF (by 13.25%) and RF (by 14.98%) lunges, and smallest contact pressure is found in the RB (by 29.61%) lunge.

### 3.3. von Mises Stress

To facilitate illustration of von Mises stress loadings in the femoral and patella cartilage, the peak values at the contact surface and chondral surface are presented in Fig. 6. In terms of the peak von Mises stress at the contact surface, the LF lunge presents 9.5 MPa in the femoral cartilage and 10.02 MPa in the patella cartilage, respectively. While peak stress values of 9.64 MPa and 13.99 MPa are observed in the chondral surface of the femoral and patella cartilage. As for the LB lunge, peak values of 11.28 MPa (femoral cartilage) and 11.23 MPa (patella cartilage) are reported at the contact surface, while 10.73 MPa and 16.3 MPa at the chondral surface are observed in the femoral and patella cartilage, respectively. The RF lunge shows peak von Mises stress of 9.25 MPa (femoral cartilage) and 9.02 MPa (patella cartilage) at the contact surface, and 9.31 MPa (femoral cartilage) and 12.57 MPa (patella cartilage) at the chondral surface. The RB lunge exhibits peak von Mises stress values of 7.88 MPa (femoral cartilage) and 8.12 MPa (patella cartilage) at the contact surface, and 8.1 MPa (femoral cartilage) and 11.08 MPa (patella cartilage) in the chondral surface.

The peak von Mises stresses in the contact femoral cartilage were 11.28 MPa (LB), 9.5 MPa (LF), 7.88 MPa (RB) and 9.25 MPa (RF), respectively. The largest von Mises stress is observed in the LB lunge, with 13.1% reduced stress in the LF lunge, 17.99% reduced stress in the RF lunge, and 30.1% reduced stress in the RB lunge. The peak stress values on the patella cartilage were 16.3 MPa (LB), 13.99 MPa (LF), 11.08 MPa (RB) and 12.57 MPa (RF), respectively. The largest von Mises stress is found in the LB lunge, followed by reductions of 14.17% and 22.88% in the LF and RF lunges, respectively, and 32.02% reduction in the RB lunge.

In general, the overall von Mises stress distribution patterns reveal that the LB lunge presents the largest stress loading in the cartilage, followed by the LF and RF lunges, and finally the RB shows the smallest stress loading. At the contact surface, the patella cartilage has greater loading than the femoral cartilage, while the chondral surface presents larger von Mises stress loadings than the contact surface.

Fig. 7 further illustrates the von Mises stress pattern in the cartilage of the anterior-posterior intersection of the patellofemoral groove at the mid-point and max location. The LF presents stress loading of 9.51 MPa, followed by the RF lunge of 8.98 MPa and RB lunge of 8.75 MPa, and the least with 8.46 MPa in the LB lunge. The largest maximal von Mises stress is in the LF lunge (17.61 MPa), followed by the LF lunge (15.2 MPa), RF lunge (12.72 MPa) and RB lunge (11.08 MPa).

**Table 1**
The input parameters of knee flexion angle and quadricep muscle forces (in Newton and normalized body weight) for FE simulation.

| | Right-forward | Left-forward | Right-backward | Left-backward |
|---|---|---|---|---|
| Knee Angle | 65° | 79° | 60° | 63° |
| VM | 640 N (0.95BW) | 650 N (0.97BW) | 450 N (0.67BW) | 760 N (1.13BW) |
| VI | 686 N (1.02BW) | 690 N (1.03BW) | 585 N (0.87BW) | 886 N (1.32BW) |
| RF | 732 N (1.09BW) | 785 N (1.17BW) | 605 N (0.9BW) | 850 N (1.26BW) |
| VL | 1178 N (1.75BW) | 1380 N (2.06BW) | 908 N (1.35BW) | 1580 N (2.35BW) |

## 4. Discussion

This study aimed to investigate the loadings in the patellofemoral cartilage during directional (right-forward, RF; right-backward, RB; left-forward, LF; and left-backward, LB) lunging steps using lab tests, musculoskeletal (OpenSim) rigid body modelling and computational Finite Element (FE) simulation. The experimentally measured knee position (femur-tibia angle) and musculoskeletal-modelled quadriceps muscle forces were input as boundary conditions and loads to run the FE simulation. The hypothesis was supported with findings that the left-side (LF and LB) lunges had higher cartilage loadings compared to the right-side (RF and RB) lunges. Specifically, the largest von Mises stress loadings were observed in the LB lunge compared to LF, RF and RB lunges, while the RB lunge exhibited the smallest stress in the cartilage. Further, the chondral layer had greater loading than the contact interface, particularly the patella cartilage exhibited higher loading than the femoral cartilage.

The current study employed several indirect approaches to validate and evaluate the musculoskeletal model and FE computational model, including comparison of tibiofemoral joint (knee flexion) angles against recent studies [1,6,39], contact area between femoral and patella cartilage with recently reported contact areas of 500–600 $mm^2$ [24] and estimated peak activations of quadriceps muscles (as presented in Fig. 4). However, the quadriceps forces during badminton lunges are rarely reported in the literature, though a recent study utilized the musculoskeletal modelling technique to estimate the contact force in the joints of the lower extremity [40], but the force values were not reported. In this study, the discrete quadriceps (VM, VL, VI and RF combined) forces used for RF, RB, LF and LB lunges were 3236 N (4.82BW), 2548 N (3.79BW), 3505 N (5.22BW), and 4076 N (6.07BW), while compared to the mean quadriceps force of 3.3 BW in the stair climbing

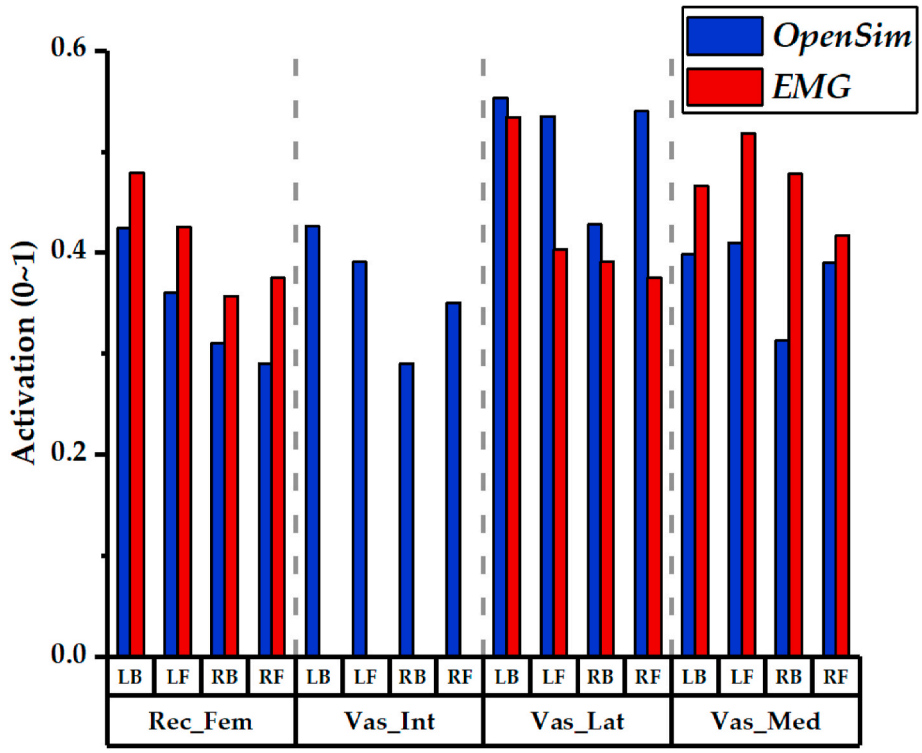


**Fig. 4.** Comparison of estimated peak OpenSim activations against EMG recorded signals. Rec_Fem: rectus femoris, Vas_Int: vastus intermedius, Vas_Lat: vastus lateralis and Vas_Med: vastus medialis, and LB, LF, RB and RF represents Left-Backward, Left-Forward, Right-Backward and Right-Forward lunges, respectively.

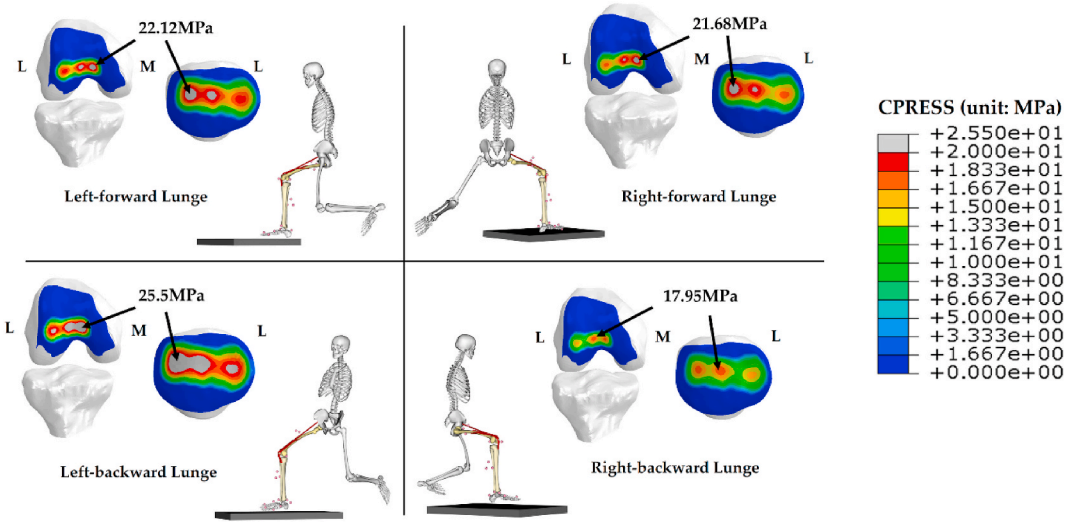


**Fig. 5.** Distribution of contact pressure on the femoral cartilage and patella cartilage.

study with contact pressure around 4 MPa [23,25,35]. The higher contact pressure from the current study may be from greater quadriceps muscle forces. It should be further noted that the mean approaching speed was ~3.0 m/s (maximal speed up to ~4.5 m/s) from the four directional lunges, which explained the larger contact pressure from the higher lunging speed (more dynamic) compared to the stair ascending and squatting [25,35] tasks. As reported, the higher speed would result in greater magnitude of impact to the lower extremity [40,41].

Recent studies compared the kinetics in the four directional lunges, and reported that the left-forward (LF) lunges had increased peak loading, loading rate and total foot pressures; whilst, the LB showed the lowest impact and pressures [5]. Specifically, larger transverse moments but less frontal moments in the lower extremity were documented in the backhand (LF) lunge [42]. From the tactical perspective, the backhand sides (especially the back court) are the most vulnerable sites that badminton athletes tend or have been adapted to move faster towards the left-side positions to return the shuttle, thus lunging speeds and musculature activations are greater than the forehand (right) side. These was supported with consistent loading profiles in a recent review study [27], though the lunges were performed in a lab-simulated badminton court either involved with shuttle or without, which may affect the kinematic performance. While considering the contribution of quadriceps muscles estimated from the musculoskeletal modelling, the left-side (forward and backward) lunges presented larger force magnitude compared to the right-side (forward and backward) lunges. These may be explained by the higher contact pressure and von Mises stress in the

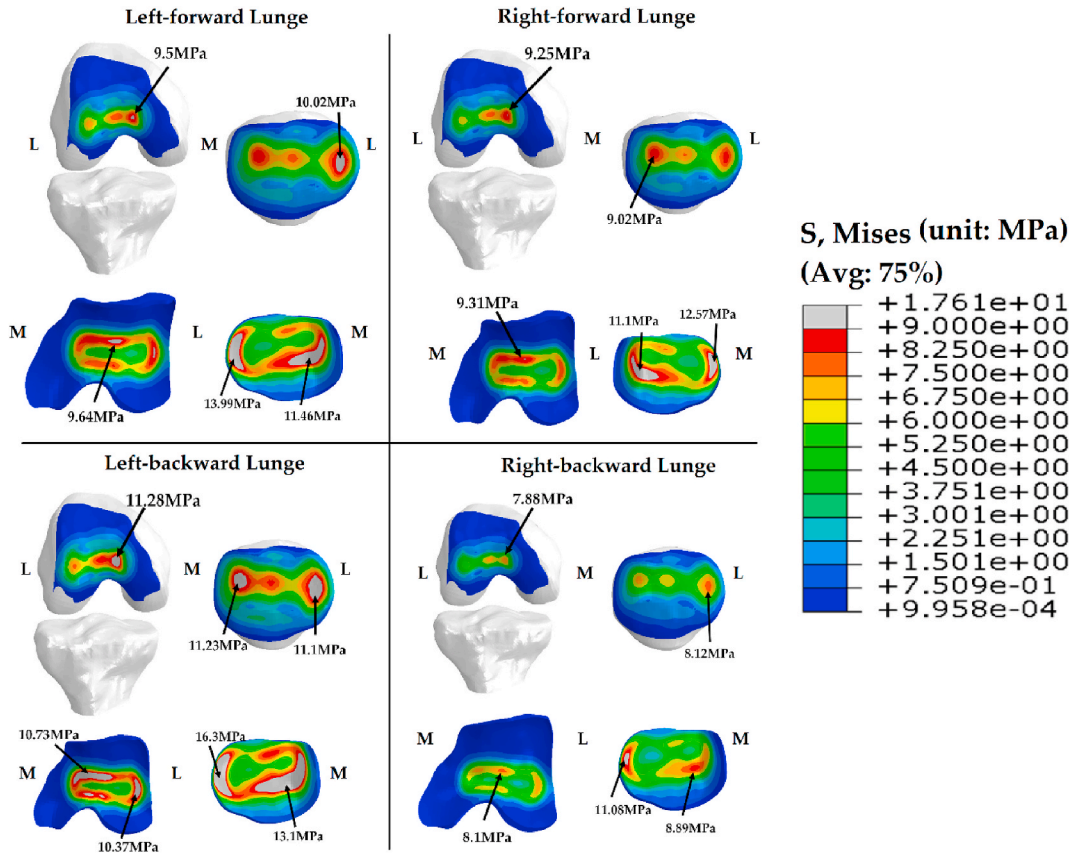


**Fig. 6.** Distribution of von Mises Stress in the contact surface (above) and chondral surface (below) of the femoral cartilage and patella cartilage with highlighted peak values.

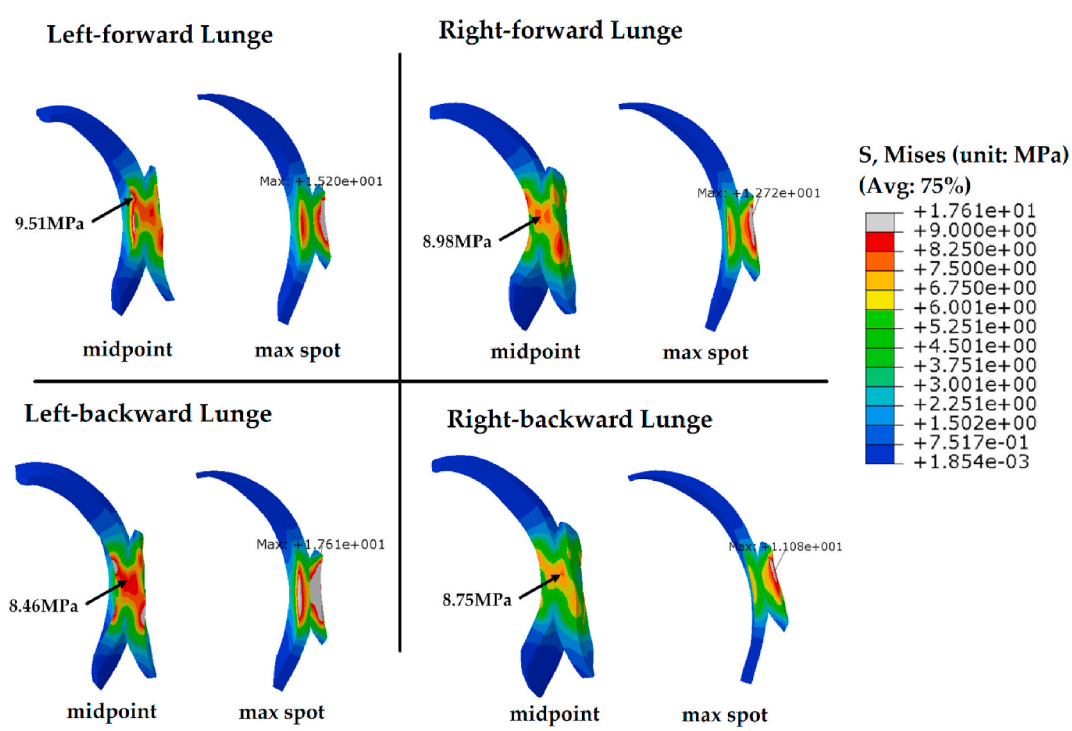


**Fig. 7.** Illustration of von Mises Stress at the cross-sectional interface (midpoint, left) of the patellofemoral groove and highlighted max location (right).

patellofemoral cartilage predicted from the current model. Specifically, the vastus lateralis (VL), rectus femoris (RF) and vastus intermedius (VI) showed greater variations across the four directional lunges, particularly larger in the left-side, which may further support the findings that primary contact loadings were observed in the medial and lateral facets of the cartilage. This information may suggest higher risk of anterior knee pain in the relevant regions [43,44].

From the authors' knowledge, this study is the first investigation exploring the patellofemoral cartilage loading during badminton lunges, and we adapted the framework integrating experimental measurement, musculoskeletal modelling, and FE simulation [23]. It was observed from the FE analysis that the contact pressure and von Mises stress from the LB lunge are greater than the LF lunge by ~13% and ~10%, respectively, which were opposite with the impact loadings previously reported [5,42,45]. The contact pressure in the femur and patella articulating surface showed similar magnitude and pattern. While comparing the results from the current model and considering the difference in the loading profiles of the left (backhand) and right (forehand) lunges with experimental studies, several points should be taken into account. For example, the computational modelling of the patellofemoral complex should consider the joint shape, quadriceps forces (the applied loads in this study), and tissue properties assigned [46]. The contact pressure and von Mises stress in the LF lunge were larger than those in the RF and RB lunges, similar with the kinetic parameters observed in recent experimental studies [5,42,45]. The von Mises stress at the contact interface of the femoral and patella cartilage showed subtle differences in the four directional lunges.

To further reveal the patellofemoral joint loading, we also quantified the stress in the cartilage from the chondral layer of the femur and patella bones, as loading in this interface was previously reported to be related with patellofemoral pain and cartilage injuries [43,44]. Consistent with the 'hot spot' region to the medial aspect of both cartilages [44], peak von Mises stress were observed in the medial aspect in the four directional lunges. What deserves special attention was that the von Mises stress on the chondral layer was higher, especially in the patella cartilage, which might suggest that this layer of patella cartilage was loaded most and susceptible to pain or tissue degeneration.

The current study explored the distribution patterns of contact pressure and von Mises stress in the patellofemoral cartilage during four directional badminton lunges. Although no statistics were reported, this was due to the fact that we employed the averaged boundary condition (mean tibiofemoral joint position) and loads (mean quadricep forces) from one participant to run the simulation. We were primarily aimed to investigate the loading patterns and distribution on the interface and within the cartilage tissues as an exploratory and perspective study, which was shown to be reliable and plausible. The findings provided additional knowledge of the cartilage loading, apart from commonly employed experimental measurement or musculoskeletal modelling.

Several limitations should be considered while interpreting the primary findings from the current study. Firstly, this study included male badminton players as participants in the experiments and computational simulation, while females with a high ratio of anterior knee (patellofemoral joint) pain are reported in the literature and might present different biomechanical features [46–48]. Thus, findings may not be applicable to the cohort of female badminton athletes. Secondly, while developing the FE model of the patellofemoral joint, a few assumptions were made for the material properties. Specifically, the cartilage was modelled as a uniform isotropic and linearly elastic material. These could be justified while mimicking activities with loading frequencies larger than 0.01Hz [36,49]. The cartilage was assigned with Young's Modulus of 12 MPa and Poisson's ratio of 0.46 [25,36]; whilst several other patellofemoral FE models used slightly different properties [35,50], it was difficult to use a uniform property, as the material properties of the patellofemoral cartilage may be different across participants [49,51]. The model did not include medial and lateral patellofemoral ligaments which might affect the contact loading in the patellofemoral cartilage. It was also difficult to perform validation for this model while we employed several indirect validations to evaluate our model, such as validation of input parameters (knee angles and quadriceps activations) and contact area. The rotation of the femur and tibia bones may also affect the loadings as reported [37,46]; however, we primarily focused the influence of quadriceps muscle forces and knee flexion position on patellofemoral loading in this study. Thirdly, it should be noted that parameters were computed from musculoskeletal modelling and from experimental tests in a lab-simulated court, which may not represent the highly dynamic situations during 'real-scenario' training or competition. Lastly, the shape (geometry) variations in the bones and cartilage were not considered [49,52] in the participant-specific patellofemoral model, as this study primarily aimed to evaluate tissue loading response and patterns in the four directional lunges. Recent presentations of statistical shape modelling [53] should be considered for future badminton related sport investigations.

## 5. Conclusion

This study conducted an exploratory investigation of the loading of the patellofemoral cartilage during directional badminton lunges integrating approaches of musculoskeletal modelling and Finite Element simulation. Consistent with current kinetic profiles of badminton lunges, the left-sided (left-forward and left-backward) backhand lunges exhibited greater loading in the patellofemoral joint. The current study also added two key findings that, 1) the left-backward lunge showed larger tissue loading in the cartilage of the right knee than left-forward lunge; and 2) the chondral layer of patellofemoral cartilage was loaded the most. This knowledge of tissue loading may have implications for the training of badminton footwork, such as musculature development, to reduce cartilage loading accumulation, and prevent potential anterior knee pain.

## Funding

This project was supported by the Badminton World Federation Sports Science project (2018–2020), Loudi Vocational and Technical College, and K. C. Wong Magna Fund in Ningbo University.

## Declaration of competing interest

We declare that we have no financial and personal relationships with other people or organizations that can inappropriately influence our work, there is no professional or other personal interest of any nature or kind in any product, service and/or company that could be construed as influencing the position presented in, or the review of, the manuscript entitled, "An Exploratory Investigation of Patellofemoral Joint Loadings during Directional Lunges in Badminton".

## References

[1] G. Kuntze, N. Mansfield, W. Sellers, A biomechanical analysis of common lunge tasks in badminton, J. Sports Sci. 28 (2010) 183–191, https://doi.org/10.1080/02640410903428533.
[2] R. Valldecabres, C.A. Casal, J.G.C. Chiminazzo, A.M. de Benito, Players' on-court movements and contextual variables in badminton World championship, Front. Psychol. 11 (2020) 1567, https://doi.org/10.3389/fpsyg.2020.01567.
[3] M. Phomsoupha, L. Guillaume, The science of badminton: game characteristics, anthropometry, physiology, visual fitness and biomechanics, Sports Med. 45 (2015) 473–495, https://doi.org/10.1007/s40279-014-0287-2.
[4] A. Lees, Science and the major racket sports: a review, J. Sports Sci. 21 (2003) 707–732, https://doi.org/10.1080/0264041031000140275.
[5] Y. Hong, S.J. Wang, W.K. Lam, J.T.M. Cheung, Kinetics of badminton lunges in four directions, J. Appl. Biomech. 30 (2014) 113–118, https://doi.org/10.1123/jab.2012-0151.
[6] Q. Mei, Y. Gu, F. Fu, J. Fernandez, A biomechanical investigation of right-forward lunging step among badminton players, J. Sports Sci. 35 (2017) 457–462, https://doi.org/10.1080/02640414.2016.1172723.

[7] W.K. Lam, R. Ding, Y. Qu, Ground reaction forces and knee kinetics during single and repeated badminton lunges, J. Sports Sci. 35 (2017) 587–592, https://doi.org/10.1080/02640414.2016.1180420.
[8] M.D. Chard, S.M. Lachmann, Racquet sports–patterns of injury presenting to a sports injury clinic, Br. J. Sports Med. 21 (1987) 150–153, https://doi.org/10.1136/bjsm.21.4.150.
[9] U. Jérgensen, S. Winge, Epidemiology of badminton injuries, Int. J. Sports Med. 8 (1987) 379–382, https://doi.org/10.1136/bjsm.24.3.169.
[10] A.H. Shariff, J. George, A.A. Ramlan, Musculoskeletal injuries among Malaysian badminton players, Singap. Med. J. 50 (2009) 1095–1097.
[11] C. Couppé, M. Kongsgaard, P. Aagaard, A. Vinther, M. Boesen, M. Kjær, S. P. Magnusson, Differences in tendon properties in elite badminton players with or without patellar tendinopathy, Scand. J. Med. Sci. Sports 23 (2013), https://doi.org/10.1111/sms.12023 e89–e95.
[12] A.P. Boesen, M.I. Boesen, M.J. Koenig, H. Bliddal, S. Torp-Pedersen, H. Langberg, Evidence of accumulated stress in Achilles and anterior knee tendons in elite badminton players, Knee Surgery, Sport, Traumatol. Arthrosc. 19 (2011) 30–37, https://doi.org/10.1007/s00167-010-1208-z.
[13] J. Cronin, P.J. McNair, R.N. Marshall, Lunge performance and its determinants, J. Sports Sci. 21 (2003) 49–57, https://doi.org/10.1080/0264041031000070958.
[14] S.J. Maloney, A review of the badminton lunge and specific training considerations, strength cond, J 1 (2018), https://doi.org/10.1519/SSC.0000000000000378.
[15] J. Jin, E. Jones, Patellofemoral pain, Jama 319 (2018) 418, https://doi.org/10.1001/jama.2017.19690.
[16] K.M. Crossley, M.J. Callaghan, R. Van Linschoten, Patellofemoral pain, BMJ 351 (2015) h3939, https://doi.org/10.1136/bmj.h3939.
[17] J.E. Taunton, M.B. Ryan, D.B. Clement, D.C. McKenzie, D.R. Lloyd-Smith, B. D. Zumbo, A retrospective case-control analysis of 2002 running injuries, Br. J. Sports Med. 36 (2002) 95–101, https://doi.org/10.1136/bjsm.36.2.95.
[18] K.M. Crossley, M.J. Callaghan, R. Van Linschoten, Patellofemoral pain, Br. J. Sports Med. 50 (2016) 247–250, https://doi.org/10.1136/bjsports-2015-h3939rep.
[19] J.K. Loudon, Biomechanics and pathomechanics of the patellofemoral joint, Int. J. Sports Phys. Ther. 11 (2016) 820–830, https://doi.org/10.1293/tox.25.37.
[20] G. Fekete, B.M. Csizmadia, M.A. Wahab, P. De Baets, L.V. Vanegas-Useche, I. Bíró, Patellofemoral model of the knee joint under non-standard squatting, Dyna 81 (2014) 60–67.
[21] J.J. Elias, A.J. Cosgarea, Computational modeling: an alternative approach for investigating patellofemoral mechanics, Sports Med. Arthrosc. 15 (2007) 89–94, https://doi.org/10.1097/JSA.0b013e31804bbe4d.
[22] J.J. Elias, D.R. Wilson, R. Adamson, A.J. Cosgarea, Evaluation of a computational model used to predict the patellofemoral contact pressure distribution, J. Biomech. 37 (2004) 295–302, https://doi.org/10.1016/S0021-9290(03)00306-3.
[23] T.F. Besier, G.E. Gold, G.S. Beaupré, S.L. Delp, A modeling framework to estimate patellofemoral joint cartilage stress in vivo, Med. Sci. Sports Exerc. 37 (2005) 1924–1930, https://doi.org/10.1249/01.mss.0000176686.18683.64.
[24] T.F. Besier, C.E. Draper, G.E. Gold, G.S. Beaupre, S.L. Delp, Patellofemoral joint contact area increases with knee flexion and weight-bearing, J. Orthop. Res. 23 (2005) 345–350.
[25] T.F. Besier, S. Pal, C.E. Draper, M. Fredericson, G.E. Gold, S.L. Delp, G.S. Beaupré, The role of cartilage stress in patellofemoral pain, Med. Sci. Sports Exerc. 47 (2015) 2416–2422, https://doi.org/10.1249/MSS.0000000000000685.
[26] J.J.J. Lee, W.P. Loh, A state-of-the-art review on badminton lunge attributes, Comput. Biol. Med. 108 (2019) 213–222, https://doi.org/10.1016/j.compbiomed.2019.04.003.
[27] W. Lam, D.W. Wong, W.C. Lee, Biomechanics of lower limb in badminton lunge: a systematic scoping review, PeerJ 8 (2020), e10300, https://doi.org/10.7717/peerj.10300.
[28] W.K. Lam, K.K. Lee, S.K. Park, J. Ryue, S.H. Yoon, J. Ryu, Understanding the impact loading characteristics of a badminton lunge among badminton players, PloS One 13 (2018), e205800, https://doi.org/10.1371/journal.pone.0205800.
[29] C.-F. Lin, S.-H. Hua, M.-T. Huang, H.-H. Lee, J.-C. Liao, Biomechanical analysis of knee and trunk in badminton players with and without knee pain during backhand diagonal lunges, J. Sports Sci. 33 (2015) 1429–1439, https://doi.org/10.1080/02640414.2014.990492.
[30] M.S. DeMers, S. Pal, S.L. Delp, Changes in tibiofemoral forces due to variations in muscle activity during walking, J. Orthop. Res. 32 (2014) 769–776, https://doi.org/10.1002/jor.22601.
[31] S.L. Delp, F.C. Anderson, A.S. Arnold, P. Loan, A. Habib, C.T. John, E. Guendelman, D.G. Thelen, OpenSim: open-source software to create and analyze dynamic simulations of movement, IEEE Trans. Biomed. Eng. 54 (2007) 1940–1950, https://doi.org/10.1109/TBME.2007.901024.
[32] U. Trinler, H. Schwameder, R. Baker, N. Alexander, Muscle force estimation in clinical gait analysis using AnyBody and OpenSim, J. Biomech. 86 (2019) 55–63, https://doi.org/10.1016/j.jbiomech.2019.01.045.
[33] Q. Mei, Y. Gu, L. Xiang, J.S. Baker, J. Fernandez, Foot pronation contributes to altered lower extremity loading after long distance running, Front. Physiol. 10 (2019) 573, https://doi.org/10.3389/fphys.2019.00573.
[34] F.C. Anderson, M.G. Pandy, Static and dynamic optimization solutions for gait are practically equivalent, J. Biomech. 34 (2001) 153–161, https://doi.org/10.1016/S0021-9290(00)00155-X.
[35] S. Farrokhi, J.H. Keyak, C.M. Powers, Individuals with patellofemoral pain exhibit greater patellofemoral joint stress: a finite element analysis study, Osteoarthritis Cartilage 19 (2011) 287–294, https://doi.org/10.1016/j.joca.2010.12.001.
[36] S. Pal, T.F. Besier, G.E. Gold, M. Fredericson, S.L. Delp, G.S. Beaupre, Patellofemoral cartilage stresses are most sensitive to variations in vastus medialis muscle forces, Comput. Methods Biomech. Biomed. Eng. 22 (2019) 206–216, https://doi.org/10.1080/10255842.2018.1544629.
[37] T.C. Liao, L. Yin, C.M. Powers, The influence of isolated femur and tibia rotations on patella cartilage stress: a sensitivity analysis, Clin. Biomech. 54 (2018) 125–131, https://doi.org/10.1016/j.clinbiomech.2018.03.003.
[38] A.A. Ali, S.S. Shalhoub, A.J. Cyr, C.K. Fitzpatrick, L.P. Maletsky, P.J. Rullkoetter, K. B. Shelburne, Validation of predicted patellofemoral mechanics in a finite element model of the healthy and cruciate-deficient knee, J. Biomech. 49 (2016) 302–309, https://doi.org/10.1016/j.jbiomech.2015.12.020.
[39] M.-T. Huang, H.-H. Lee, C.-F. Lin, Y.-J. Tsai, J.-C. Liao, How does knee pain affect trunk and knee motion during badminton forehand lunges? J. Sports Sci. 32 (2014) 690–700, https://doi.org/10.1080/02640414.2013.848998.
[40] T.L.W. Chen, Y. Wang, D.W.C. Wong, W.K. Lam, M. Zhang, Joint contact force and movement deceleration among badminton forward lunges: a musculoskeletal modelling study, Sports BioMech. (2020) 1–13, https://doi.org/10.1080/14763141.2020.1749720, 00.
[41] I.S. Davis, A.S. Tenforde, B.S. Neal, J.L. Roper, R.W. Willy, Gait retraining as an intervention for patellofemoral pain, Curr. Rev. Musculoskelet. Med. 13 (2020) 103–114, https://doi.org/10.1007/s12178-020-09605-3.
[42] M.H. Nielsen, J.N. Lund, W.K. Lam, U.G. Kersting, Differences in impact characteristics, joint kinetics and measurement reliability between forehand and backhand forward badminton lunges, Sport. Biomech. 19 (2020) 547–560, https://doi.org/10.1080/14763141.2018.1501086.
[43] W.W. Curl, J. Krome, E.S. Gordon, J. Rushing, B.P. Smith, G.G. Poehling, Cartilage injuries: a review of 31,516 knee arthroscopies, Arthroscopy 13 (1997) 456–460, https://doi.org/10.1016/S0749-8063(97)90124-9.
[44] T.F. Besier, C. Draper, S. Pal, M. Fredericson, G. Gold, S. Delp, G. Beaupré, Imaging and musculoskeletal modeling to investigate the mechanical etiology of patellofemoral pain, in: Altas Patellofemoral Jt., 2012, pp. 125–133.
[45] R. Valldecabres, A.M. De Benito, G. Littler, J. Richards, An exploration of the effect of proprioceptive knee bracing on biomechanics during a badminton lunge to the net, and the implications to injury mechanisms, PeerJ 6 (2018), e6033, https://doi.org/10.7717/peerj.6033.
[46] T.F. Besier, G.E. Gold, S.L. Delp, M. Fredericson, G.S. Beaupré, The influence of femoral internal and external rotation on cartilage stresses within the patellofemoral joint, J. Orthop. Res. 26 (2008) 1627–1635, https://doi.org/10.1002/jor.20663.
[47] R.T. Galloway, Y. Xu, T.E. Hewett, K. Barber Foss, A.W. Kiefer, C.A. DiCesare, R. A. Magnussen, J. Khoury, K.R. Ford, J.A. Diekfuss, D. Grooms, G.D. Myer, A. M. Montalvo, Age-dependent patellofemoral pain: hip and knee risk landing profiles in prepubescent and postpubescent female athletes, Am. J. Sports Med. 46 (2018) 2761–2771, https://doi.org/10.1177/0363546518788343.
[48] K.Y. Ho, J.H. Keyak, C.M. Powers, Comparison of patella bone strain between females with and without patellofemoral pain: a finite element analysis study, J. Biomech. 47 (2014) 230–236, https://doi.org/10.1016/j.jbiomech.2013.09.010.
[49] G. Li, O. Lopez, H. Rubash, Variability of a three-dimensional finite element model constructed using magnetic resonance images of a knee for joint contact stress analysis, J. Biomech. Eng. 123 (2001) 341–346, https://doi.org/10.1115/1.1385841.
[50] K.S. Shah, A. Saranathan, B. Koya, J.J. Elias, Finite element analysis to characterize how varying patellar loading influences pressure applied to cartilage: model evaluation, Comput. Methods Biomech. Biomed. Eng. 18 (2015) 1509–1515, https://doi.org/10.1080/10255842.2014.921814.
[51] K.E. Keenan, S. Pal, D.P. Lindsey, T.F. Besier, G.S. Beaupre, A viscoelastic constitutive model can accurately represent entire creep indentation tests of human patella cartilage, J. Appl. Biomech. 29 (2013) 292–302, https://doi.org/10.1123/jab.29.3.292.
[52] P. Cerveri, A. Belfatto, A. Manzotti, Representative 3D shape of the distal femur, modes of variation and relationship with abnormality of the trochlear region, J. Biomech. 94 (2019) 67–74, https://doi.org/10.1016/j.jbiomech.2019.07.008.
[53] A. Erdemir, T.F. Besier, J.P. Halloran, C.W. Imhauser, P.J. Laz, T.M. Morrison, K. B. Shelburne, Deciphering the "art" in modeling and simulation of the knee joint: overall strategy, J. Biomech. Eng. 141 (2019), 071002, https://doi.org/10.1115/1.4043346.